2023 IEEE/RSJ International Conference on Intelligent Robots and Systems (IROS)
October 1-5, 2023. Detroit, USA

Soft, modular, shape-changing displays with hyperelastic bubble arrays

Matthew R. Devlin[1], Tianshu Liu[1], Mengjia Zhu[1], Nathan S. Usevitch[1],
Nicholas Colonnese[1], and Amirhossein H. Memar[1]*

Abstract— **Incorporating compliance into shape-changing displays can improve their wearability and actuation modalities. While recent advances in soft actuators highlight promising paths for soft shape-changing displays, these displays currently face some practical challenges of device failure and limited actuator displacement. A monolithic fabrication processes means the device is challenging to repair, for a single point of failure often renders the whole device ineffective. We have leveraged a modular hyperelastic bubble array layer to create a soft shape-changing skin. The modularity of this device allows for rapid repair of individual bubbles and fast prototyping, and the spherical, hyperelastic actuators enable an increase in degrees of freedom due to bubble-to-bubble interactions. Furthermore, we present a forward kinematic description of our device, incorporating these bubble-to-bubble interactions and the nonlinear instabilities unique to hyperelastic actuator inflation. We demonstrate the utility of this soft shape-changing skin as a haptic display that can be worn comfortably or applied to passive interactive objects such as a computer mouse.**

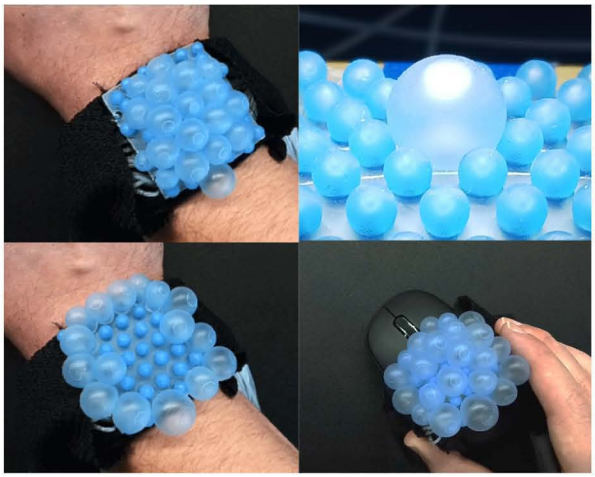

Fig. 1. An overview of the form factor and use cases for a soft shape-changing skin.

I. Introduction

Shape-changing displays are used to render digital information in the physical world. Often, they are displays with one actuator per "pixel," with an array of actuators in plane, actuating out of plane to create a 2.5D surface. Primarily, these displays use large actuators to accomplish their shape change. Previous examples have used electromechanical [1], [2], [3], [4], [5], fluidic [6], [7], and thermal actuation [8] in order to do this. Each of these approaches has its own limitations and challenges. On our goal to create a compact and wearable shape-changing display, we find a form factor limitation within the state of the art. Most shape-changing displays rely on proximate, rigid actuators or have a limited range of possible deformations.

In order to enable shape change within a soft and low-profile package, we have identified bubble arrays as a useful shape changing platform. A bubble array is a fluidically actuated device that is often used to generate fine tactile pressure. Previous work on bubble arrays including tactor manipulation [9], bubble modeling [10], [11], and integrated sensing[12], [13]. However, bubble arrays have challenges such as limited actuator displacement, and thus are not inherently well suited for shape-changing displays with demands of repeatable large displacement.

To overcome these challenges, we leverage the benefits of a hyperelastic bubble array in order to create a soft, robust approach toward a shape-changing display. By moving actuation off-body, we have created a more wearable shape-changing display. Each individual bubble within the array is individually addressable, which overcomes many degrees of freedom challenges of other wearable shape displays. The bubble arrays in [12] have a similar mechanical design: a flat, flexible membrane is fabricated on top of a series of pneumatic connections. The bubbles actuate as the bubble membrane deforms from a flat state to an approximately spherical shape with increasing pressure. However, the planar rest configuration of the bubble membrane potentially limits the amount of displacement that can be achieved due to the large strain induced during the membrane inflation. In addition, these devices are often fabricated monolithically, meaning that if a defect occurs (ex, a bubble pops or a leak forms), it can be challenging to make a repair on a single part of the device, and the entire display must be replaced.

To overcome this, we created a bubble array with hyperelastic bubbles where the bubble membrane has a spherical rest shape, as opposed to a planar rest shape. By constraining these soft bubbles to a flexible pneumatic backplane, we are able to standardize the manufacturing process to create separate actuation and pneumatic routing layers. This allows for rapid device repair and iteration which can now happen independently of pneumatic routing and control. We leverage a soft robotics approach to actuator design will enable a robust, multifunctional bubble array that is capable of shape change, with a wearable form factor that is not possible of other shape-changing displays. We propose models for both individual bubbles and multi-bubble interaction, and validate our theoretical predictions with analytical results.

We demonstrate our soft shape-changing skin in a range of

[1]Meta Reality Labs, Redmond, WA 98052.
* Corresponding author. Email: amirmemar@meta.com

2023 IEEE/RSJ International Conference on Intelligent Robots and Systems (IROS) | 978-1-6654-9190-7/23/$31.00 ©2023 IEEE | DOI: 10.1109/IROS55552.2023.10341591

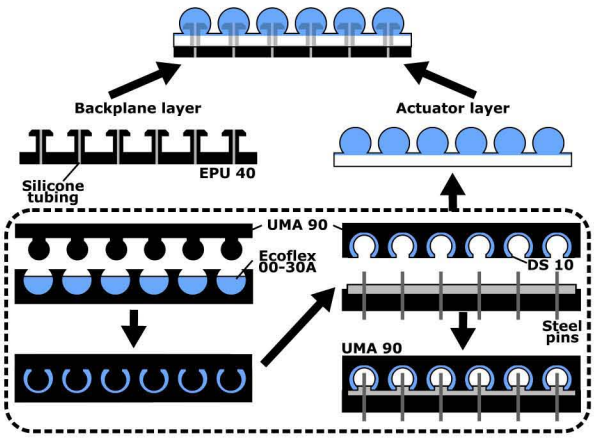

Fig. 2. Schematic of the fabrication process of the soft shape-changing skin. Materials are color coded. Blue indicates Smooth-On Ecoflex 00-30A. White indicates Smooth-On Dragonskin 10. Black represents Carbon 3D printed components in either UMA 90 or EPU 40. Gray represents steel dowels used as negative mold components.

applications including a wearable shape changing wristband and a robotic skin on mouse for interaction. Feedback gathered from a qualitative user survey indicates that our soft shape-changing skin holds promise for augmenting haptic interactions for human-computer-interaction.

The remainder of the paper will be presented in four sections. In Section II, we discuss the design concept of the soft shape-changing skin, and in Section III, the mathematical analysis of various components required to achieve the desired functionality of the device. In Section IV, we detail the fabrication of all the components of final design of soft shape-changing skin, with Section V presenting the validation of each of the chosen components.

II. Design Concept

The primary goal of this device is to be able to render a variety of surfaces, while remaining fully soft. A fully soft shape display has many use cases, and is particularly successful in a wearable context.

A. Hyperelastic actuator design

As a first step of an actuator embedded array with multiple, identical actuators, we have selected spherical volumetric actuators for their symmetry in three dimensions and ability to create bubble-bubble interactions with neighboring bubbles. Spherical bubbles, which have an initially raised spherical geometry before inflation, have a much greater lateral strain that more common planar bubble arrays, which have an initial, circular geometry that is flush against the rest of the actuator. Creating a soft, reliably spherical actuator is nontrivial and relies on precise wall thickness management. Spherical bubbles have not been shown previously in bubble arrays, due to the complexity of their manufacture. The lateral displacement of spherical bubbles also introduces challenges in the modeling of these bubble arrays due to the bubble-bubble interactions. Our goal is to take advantage of commercial silicones such as Smooth-On Ecoflex 00-30A to render large strains unseen in previous bubble arrays.

B. Multi-layer coupling

These actuators are mechanically attached to flexible substrate that allow the actuators to stay in alignment for ease of manufacture and modeling. The substrate remains flexible but inelastic which allows for the stiffness of the substrate has an effect on the behavior of the overall system. With a large array of identical units, this mesh has many redundant units that may go underutilized for specific applications. Pragmatically, separating the actuation layer and the pneumatic routing layer allows for a faster prototype iteration cycle. Many soft actuators are susceptible to leaks and punctures, resulting in total device failure. By having the pneumatic routing for the array bonded to a separate layer, the actuators can be replaced on the fly, rather than a single bubble puncture resulting in a total device failure in chemically bonded systems.

C. Individual bubble control

To create a shape changing array, it is important to have a description for the shape change of a single unit. In this work, we detail a forward kinematic approach of pneumatic control to generate the desired bubble volume change and vertical displacement. We also take into account the effects of neighboring bubbles, and show that the degrees of freedom of the system can be extended by incorporating an order-dependence in our model.

III. Modeling

A. Individual bubble shape control modeling

To describe the kinematics of a spherical membrane, we define the spherical coordinate system using the standard (r,θ,ϕ) system. Then, we can define the unit vectors as

$$e_\theta = \frac{\partial x}{\partial \theta}, e_\phi = \frac{\partial x}{\partial \phi}, n = \frac{\partial x}{\partial r}. \tag{1}$$

Under uniform pressure, the membrane will be under bi-axial stretch everywhere. Assuming the membrane material is in-compressible, the deformation gradient tensor can be written as

$$F = \lambda \left(e_\theta e_\theta + e_\phi e_\phi\right) + \frac{1}{\lambda^2} nn. \tag{2}$$

where $\lambda = \frac{r}{r_0}$. The membrane is a type of silicone, so we assume it can be described by in-compressible Yeoh model where the energy density function can be written as

$$\begin{aligned} W(F) = \frac{\mu}{2}(I(F)-3) + C_2(I(F)-3)^2 \\ + C_3(I(F)-3)^3 - \alpha(J-1) \end{aligned} \tag{3}$$

where I is the first invariant of $B = FF^T$, μ is the Young's modulus of the material, and α is the Lagrange Multiplier for volume conservation. The Cauchy stress can be calculated as

$$\sigma = \frac{1}{J}\frac{\partial W}{\partial F}F^T = \frac{2}{J}B\frac{\partial W}{\partial I} - \alpha 1 \tag{4}$$

Where 1 is the unity tensor. Substitute (2) to (4) and together with the incompressibility condition $J = 1$, we get

$$\sigma = \left(2\lambda^2 - \alpha\right)\frac{\partial W}{\partial I}\left(e_\theta e_\theta + e_\phi e_\phi\right) + \left(\frac{2}{\lambda^4} - \alpha\right) nn \quad (5)$$

The normal component of the Cauchy stress has to be zero, therefore, $\alpha = \frac{2}{\lambda^4}$, and the Cauchy stress is

$$\sigma = 2\left(\lambda^2 - \frac{1}{\lambda^4}\right)\frac{\partial W}{\partial I}\left(e_\theta e_\theta + e_\phi e_\phi\right) \quad (6)$$

Then the pressure required to inflate the membrane can be calculated as

$$P = \frac{2\sigma h}{r} = 4\frac{\partial W}{\partial I}\frac{h_0}{r}\left(1 - \frac{1}{\lambda^6}\right) \quad (7)$$

Where P is the internal pressure, h_0 is the initial thickness of the membrane, and h is the deformed thickness of the membrane. We can fit with the experimental data using the relation above. The parameters from the fit are $\mu = 39.62kPa$, $C_2 = 417.3Pa$, $C_3 = 60.65Pa$. As seen in Fig. 4, we use this model to predict the height of an individual bubble.

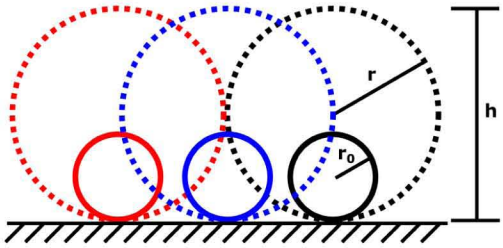

Fig. 3. The geometric model for two interacting bubble actuators. Where r_0 is the initial radius of a single bubble, r is the radius of a single bubble, and h is the height that the bubble as measured from the baseplane.

B. Multi-bubble interaction model

To understand the order-dependence on bubble inflation, we assume that the bubbles are rigid, expanding spheres such that

$$r_{bubble} \leq d - r_{neighbor} \quad (8)$$

Where a r_{bubble} is the radius of an inflating bubble, d is the center to center distance between two bubbles, and $r_{neighbor}$ is the radius of the neighboring bubble.

This simplistic multi-bubble interaction model predicts contact between bubbles and assumes that neighbor contact restricts further growth for the smaller bubble.

IV. Fabrication

The fabrication of spherical actuators embedded into a single casting process has not been previously demonstrated.

A. Actuator layer

The fabrication process of the actuation layer is a two step molding process that uses a total of three components. In Fig. 2 we visualize the process of making the silicone actuation layer. First, an array of 3D printed (Carbon M2, Urethane Methacrylate 90) spherical wells are filled with Smooth-On Ecoflex 00-30A, dyed blue for identification. A second 3D printed piece (Carbon M2, Urethane Methacrylate 90) is stacked on top in order to cast the hollow cavity within the spheres. The wall thickness of these Ecoflex 00-30A spheres is 1mm with a sphere diameter of 5mm. To increase the cure speed of this process, the parts are cured in an oven at 80 °C for 20 minutes.

After the blue Ecoflex 00-30A portion is cured, the inner mold of the spheres is removed. This will then become the top piece of the second molding step. To prepare the bottom piece, Smooth-On Dragonskin 10 is cast into a square well perforated with steel dowel pins. The pins interlock with the spherical shells cast previously, in order to ensure that there is a consistent air channel into each actuator. These two pieces, the cured, blue Ecoflex 00-30A part, and the well of Dragonskin 10, are pressed together and cured in the oven at 80 °C for 10 minutes. A shorter oven time is possible due to the thermal conductivity of the steel dowel pins. After curing, the silicone pieces can be removed with from the mold as a single, complete actuation layer.

It is worth noting that the plane of Dragonskin 10 is intentionally stiffer in order to isolate the strain of the bubble actuation to the sphere itself and not the connection point to the pneumatic routing. In addition, the steel dowel pin diameter must be significantly undersized from the backplane barb diameter, so that the elasticity of the actuation layer can serve as the primary mechanical attachment. This non-uniform stiffness within the actuation layer is a key feature that enables the modularity of the rest of the system.

B. Pneumatic backplane layer

The backplane layer is where the pneumatic routing is bonded and attached to a pneumatic manifold. Flexible barbs are 3D printed on a Carbon M2 with EPU 40. In order to ensure no leaks in the pneumatic routing, 1mm OD silicone tubing was threaded through each barb to create individually addressable pneumatic connections. The pneumatic manifold is comprised of Festo VEAB, 1-200kPa pressure regulators and a National Instruments cDAQ-9174 with a NI9264 module that can be commanded via a custom MATLAB interface. Individual actuators are delivered pressure using a closed, PID control loop to ensure an accurate pressure.

The actuator and backplane layers can be combined through press fit connections. The actuator layer intentionally has enough elasticity to fit over the larger barbs of the backplane layer while the restoring force holds the actuator tightly to the barb. Interestingly, when the actuators are overinflated, instead of rupturing, the actuator simply slips off of the barb. This is a useful feature in order to preserve the lifespan of the actuators. Intentional, nondestructive failure

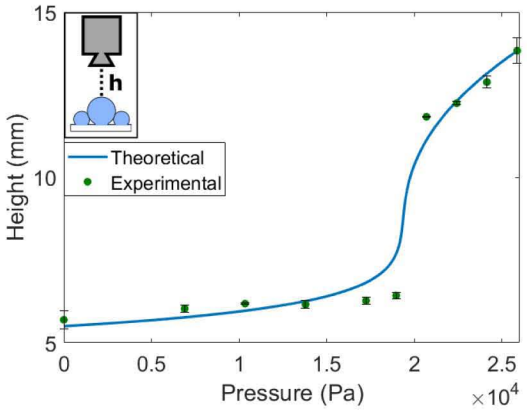

Fig. 4. Single bubble height as a function of pressure with the derived model included as the dashed line. Height was measured with a Keyence 7000 and repeated in triplicate.

modes should be considered in silicone actuator designs when possible.

V. System Validation and Performance

A. Individual bubble control

We characterize the ability of our model to predict the height of our bubble across a range of pressures. Using the ZStack function on a Keyence 7000 microscope, we are able to precisely measure the individual bubble height as a function of pressure. In Fig. 6 we see the model is closely followed by the experimental data. Importantly, the model is able to predict the location of the instability, and the general performance of the actuator on either side of the nonlinearity. Experiments were run in triplicate with minimal error in sample height on the same bubble.

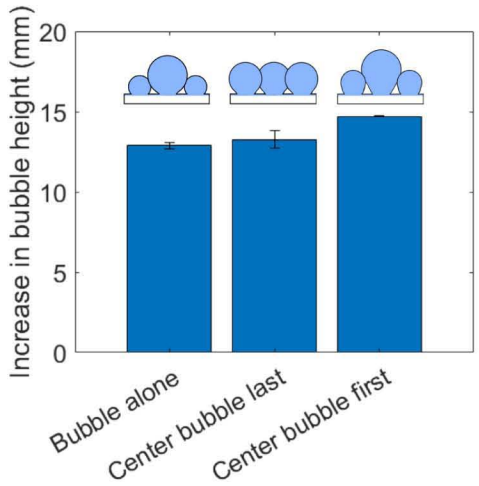

Fig. 5. The effect of inflation order on the maximum possible height of the bubble. It is possible to get a significant increase in bubble height if the surrounding bubbles are inflated after the bubble of interest. Bubble height was measured on a Keyence 7000 and repeated in triplicate.

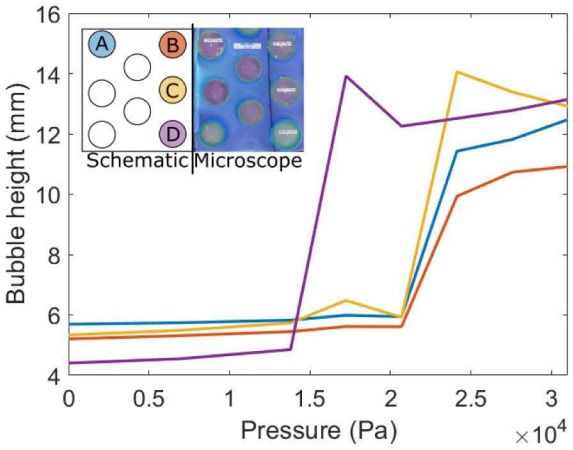

Fig. 6. A variety of measured bubble heights on a single actuation layer. All heights were measured concurrently as a function of inflation pressure. While many of the bubbles have a similar inflation curve, it is worth noting that it is not entirely homogeneous across the sample. We believe that this can be improved with stiffer casting molds and fabrication processes.

B. Order dependence

The order dependence of this work is enabled by the hyperelasticity of each individual actuator. Since each actuator is able to make contact with its neighbor, inflation constraints are tied to neighbor inflation states. Some intuition is gathered in our original model in Eq. 8, where contact between neighboring actuators could restrict growth. We observe that in an experiment where a single bubble is inflated on the actuator, as seen in the top right of Fig. 1, a single bubble can reach a height of approximately 12mm. If this bubble first has a ring of constraining bubbles inflated around it, is is still able to inflate to the unconstrained height due to the natural compliance of the system. However, if the center bubble is inflated first, and then the ring of constraining bubbles is inflated around it, the center bubble is lifted farther and experiences a significant increase in total height, around 14mm.

C. Demonstrations

To demonstrate the applications of this work, we show three possible interaction scenarios. The first is a pulsing gesture that can be worn on the wrist. This is a sequence of an inner circle and an outer ring oscillating between maximum inflation states. This generates a dramatic pulse that can be felt with the opposite hand. This pulse can be tied to a notification or any other alert.

Next, the soft shape-changing skin can be applied to a passive surface, such as a computer mouse. Using the mouse pointer coordinates, we are able to interact with a 3D topological surface on the computer. The mouse remains usable when the device is not activated, because it is naturally soft and compliant. However, the large inflation when moving the cursor across the 3D landscape provides an intuitive method of finding the peaks and valleys of a surface.

Lastly, we created an activity where the user can mouse over a digital representation of the array and activate indi-

vidual units. This allows for digital buttons to be generated on the surface which allows for further human-computer interaction.

D. User feedback

We asked 8 participants to interact with and test the soft shape-changing skin as part of a pilot assessment. Each participant was able to freely feel the device, before testing two of the different demonstration modes of the device. When asked about the feeling of the device itself, feedback was generally positive. According to P1: *They were VERY malleable and comfortable. Reminded me of stress balls and silicone kids' toys.* however, another participant found the silicone layer to be interesting, but asked if it would *be possible to play with the surface texture in order to change the sensation*. One suggestion was to *cover the surface with fabric so it is not as squishy.*

The over 50% of participants rated the feel of the haptic sensations to be "pleasant" and "strong." When asked about the ease of localizing the sensation produced by the actuator, the participants were presented with two modes: pulsing and topology rendering. A "pulse" was an oscillation between the inner bubbles and the outer bubbles of the device. The topology rendering, was experienced by placing the device on a computer mouse, and navigating a simulated terrain. All participants said that it was easiest to differentiate between the inner and outer rings of the pulsing gestures. One participant even specified that it was *challenging to differentiate between some of the features on the surface* for the topological rendering case.

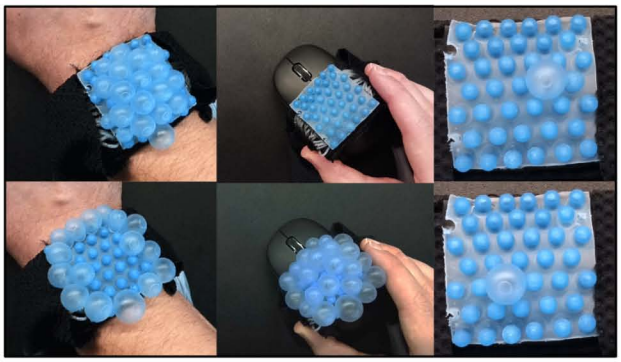

Fig. 7. A range of demonstrations possible with this soft shape-changing skin. Before and after are on top and bottom respectively. The left column is a pulsing gesture where the center bubbles inflate together, and then the outer "framing" bubbles inflate sequentially. In the middle column is the device applied to a computer mouse. A computer can relay mouse coordinates in order to display 3D data on the bubble array by prescribing a pressure. On the right column is a demonstration of individual bubble actuation and control.

VI. Conclusions and Future Work

This work demonstrates a proof-of-concept soft shape-changing skin that is capable of robust shape change while remaining fully soft. The fabrication of separate actuation and pneumatic routing layers is unique and scalable. We present a forward kinematic model of this array, and some applications that highlight the ability of the array to interact with the user.

Future versions of this work will have a normal and shear force description and quantitative user studies to understand perception. In addition, finer topological rendering and more modular actuator layers are of particular interest. Using this design as a platform for rapidly interchangeable actuation layers could see an increase in iteration speed for prototyping multiactuator soft systems. Leveraging the modularity in order to create non-uniform interaction surfaces remains an interesting design space that is unexplored.

References

[1] S. Follmer, D. Leithinger, A. Olwal, A. Hogge, and H. Ishii, "inFORM: dynamic physical affordances and constraints through shape and object actuation," in *Proceedings of the 26th annual ACM symposium on User interface software and technology*. St. Andrews Scotland, United Kingdom: ACM, Oct. 2013, pp. 417–426. [Online]. Available: https://dl.acm.org/doi/10.1145/2501988.2502032

[2] A. F. Siu, S. Kim, J. A. Miele, and S. Follmer, "shapeCAD: An Accessible 3D Modelling Workflow for the Blind and Visually-Impaired Via 2.5D Shape Displays," in *The 21st International ACM SIGACCESS Conference on Computers and Accessibility*. Pittsburgh PA USA: ACM, Oct. 2019, pp. 342–354. [Online]. Available: https://dl.acm.org/doi/10.1145/3308561.3353782

[3] B. Yu, N. Bongers, A. van Asseldonk, J. Hu, M. Funk, and L. Feijs, "LivingSurface: Biofeedback through Shape-changing Display," in *Proceedings of the TEI '16: Tenth International Conference on Tangible, Embedded, and Embodied Interaction*. Eindhoven Netherlands: ACM, Feb. 2016, pp. 168–175. [Online]. Available: https://dl.acm.org/doi/10.1145/2839462.2839469

[4] J. Hardy, C. Weichel, F. Taher, J. Vidler, and J. Alexander, "ShapeClip: Towards Rapid Prototyping with Shape-Changing Displays for Designers," in *Proceedings of the 33rd Annual ACM Conference on Human Factors in Computing Systems*. Seoul Republic of Korea: ACM, Apr. 2015, pp. 19–28. [Online]. Available: https://dl.acm.org/doi/10.1145/2702123.2702599

[5] A. Steed, E. Ofek, M. Sinclair, and M. Gonzalez-Franco, "A mechatronic shape display based on auxetic materials," *Nat Commun*, vol. 12, no. 1, p. 4758, Aug. 2021. [Online]. Available: https://www.nature.com/articles/s41467-021-24974-0

[6] S.-Y. Teng, T.-S. Kuo, C. Wang, C.-h. Chiang, D.-Y. Huang, L. Chan, and B.-Y. Chen, "PuPoP: Pop-up Prop on Palm for Virtual Reality," in *Proceedings of the 31st Annual ACM Symposium on User Interface Software and Technology*. Berlin Germany: ACM, Oct. 2018, pp. 5–17. [Online]. Available: https://dl.acm.org/doi/10.1145/3242587.3242628

[7] R. H. Heisser, C. A. Aubin, O. Peretz, N. Kincaid, H. S. An, E. M. Fisher, S. Sobhani, P. Pepiot, A. D. Gat, and R. F. Shepherd, "Valveless microliter combustion for densely packed arrays of powerful soft actuators," *Proc. Natl. Acad. Sci. U.S.A.*, vol. 118, no. 39, p. e2106553118, Sep. 2021. [Online]. Available: https://pnas.org/doi/full/10.1073/pnas.2106553118

[8] J. Du, P. Markopoulos, Q. Wang, M. Toeters, and T. Gong, "ShapeTex: Implementing Shape-Changing Structures in Fabric for Wearable Actuation," in *Proceedings of the Twelfth International Conference on Tangible, Embedded, and Embodied Interaction*. Stockholm Sweden: ACM, Mar. 2018, pp. 166–176. [Online]. Available: https://dl.acm.org/doi/10.1145/3173225.3173245

[9] S. Ukai, T. Imamura, M. Shikida, and K. Sato, "Bubble Driven Arrayed Actuator Device for a Tactile Display," in *TRANSDUCERS 2007 - 2007 International Solid-State Sensors, Actuators and Microsystems Conference*. Lyon: IEEE, Jun. 2007, pp. 2171–2174. [Online]. Available: https://ieeexplore.ieee.org/document/4300597/

[10] L. Kratchman, Jian Wen, M. Michener, and R. B. Gillespie, "Modeling pneumatic bubble displacements with membrane theory," in *2010 IEEE Haptics Symposium*. Waltham, MA, USA: IEEE, Mar. 2010, pp. 327–334. [Online]. Available: http://ieeexplore.ieee.org/document/5444634/

[11] T. Liu, M. Chiaramonte, A. Amini, Y. Menguc, and G. M. Homsy, "Indentation and bifurcation of inflated membranes," *Proc. R. Soc. A.*, vol. 477, no. 2247, p. 20200930, Mar. 2021. [Online]. Available: https://royalsocietypublishing.org/doi/10.1098/rspa.2020.0930

[12] J. Barreiros, I. Karakurt, P. Agarwal, T. Agcayazi, S. Reese, K. Healy, and Y. Menguc, "Self-sensing Elastomeric Membrane for Haptic Bubble Arrray," in *2020 3rd IEEE International Conference on Soft Robotics (RoboSoft)*. New Haven, CT, USA: IEEE, May 2020, pp. 229–236. [Online]. Available: https://ieeexplore.ieee.org/document/9116051/

[13] B. Zhang and M. Sra, "PneuMod: A Modular Haptic Device with Localized Pressure and Thermal Feedback," in *Proceedings of the 27th ACM Symposium on Virtual Reality Software and Technology*. Osaka Japan: ACM, Dec. 2021, pp. 1–7. [Online]. Available: https://dl.acm.org/doi/10.1145/3489849.3489857